JOURNAL OF MATERIALS SCIENCE 33 (1998) 4307–4314

Specimen size effects in the tensile failure strain of an epoxy adhesive

A. TOWSE†, K. POTTER†, M. R. WISNOM†, R. D. ADAMS‡
Departments of Aerospace† and Mechanical Engineering‡, University of Bristol, Bristol BS8 1TR, UK
E-mail: A.Towse@bristol.ac.uk

The tensile failure strain of a proprietary single-part aerospace epoxy adhesive (3M EC3448) has been investigated. Three different specimen sizes were tested, a large specimen of 1840 mm^3, a medium specimen of 125 mm^3 and a small specimen of 1.41 mm^3. A novel form of video extensometry was utilized to measure the tensile strain and Poisson's ratio of the specimens. It was seen that the stress–strain curve was common between the specimen sizes, with the strain at failure increasing as specimen size reduced. Analysis of the defects causing failure indicated a correlation between the size of the defect and the failure strain. The data from each specimen size were fitted to a two-parameter Weibull distribution with good correlation. A simple scaling chart using the characteristic failure strains from the three specimen sizes was formulated which indicated an equivalent Weibull shape factor of 7.9.

1. Introduction

The use of adhesive bonding in structural applications offers great advantages, primarily in the ease with which dissimilar materials may be joined. One of the primary difficulties in the use of adhesive bonding is the behaviour of the adhesive materials and the prediction of cohesive failure of the joint under many different environmental and testing conditions. Prediction of failure of uncracked adhesive joints under room temperature (RT) nominally dry conditions at moderate quasi-static strain rates is a difficult task, the criteria most commonly applied being a limiting stress or strain, applied either at a point [1] in the adhesive or over a region [2, 3]. Due to the non-uniform nature of the stress distributions in adhesive joints, and the fact that the joint geometry is often complex, finite element analysis (FEA) is most often employed to predict the strains and stresses to which the failure criteria are applied.

It can be seen from FEA [2] that small volumes of material close to the stress concentration points, such as the corners at the ends of the adherends, are at very high strains. Removing the mathematical singularity by introducing localized rounding is still seen to create very large strains [4], this time the strains being related to the degree of rounding rather than to the mesh density as for the singularity models. Little justification is made in the literature as to how these high tensile strains are able to be borne in the material without failure occurring. Also, the FEA predicts that small changes in local geometry cause large differences in peak strain. If peak strain is used as the failure criterion, then it should be expected that large variations in adhesive joint strength would be seen as the local geometry cannot be controlled in any practical joint. This degree of scatter in strength is not generally seen in adhesive joints [5].

The use of a stressed volume, rather than a peak stress, approach to failure prediction is capable of answering the problems outlined above. Even though some adhesive is highly strained, the probability of failure of these volumes may be lower than that of other, larger, volumes of the adhesive strained to a lesser degree, if the material is scale sensitive. The Weibull distribution is most often used for this type of analysis, with the materials under test ranging from pure unreinforced epoxy [6] to fibre-reinforced epoxies [7, 8]. A particularly extensive review of the materials which have shown a scale effect is presented by Harter [9]. All that is required for a material to exhibit scale sensitivity (the scale being either length, area or volume) is that the failure of the material is sensitive to the nature and distribution of defects within the specimen. The purpose of this investigation was to determine if the adhesive 3M EC3448 was scale sensitive.

2. Experimental procedure

2.1. Specimen geometry

To be able to measure the increasing strain to failure of specimens, a large ratio of relative volumes is generally required between the largest and smallest specimen (depending on the Weibull shape factor, *m*). The specimens used in this study are shown in Fig. 1, and the ratio of volumes is approximately 1300 : 90 : 1.

The large and medium specimens are of approximately standard shapes and the specimens are sized to ensure the ratio of gauge length to gauge width is 5 : 1 or greater. The smallest specimens have two "U"

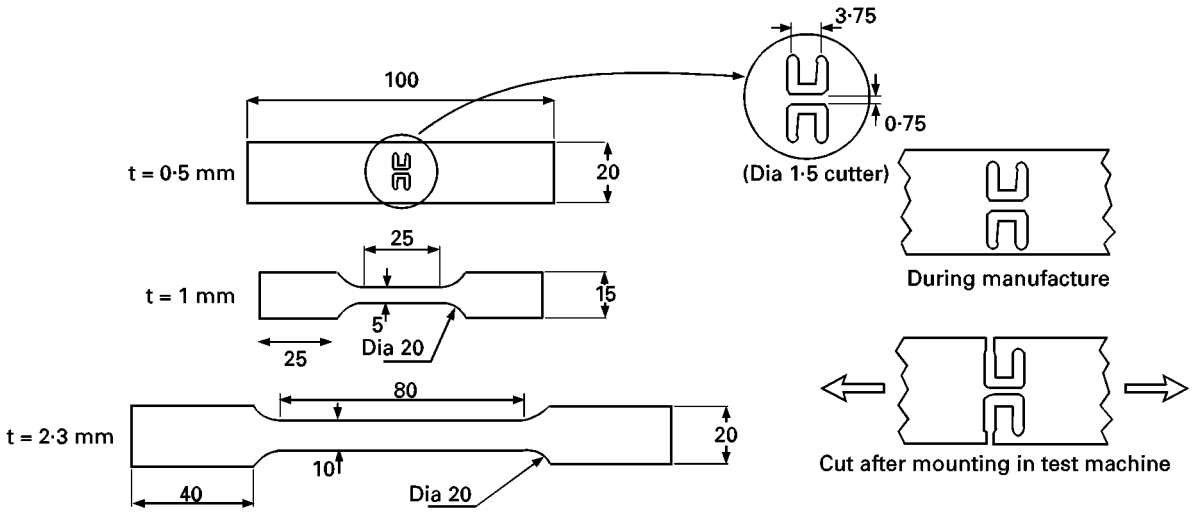

Figure 1 Nominal sizes for large, medium and small specimens (all dimensions in mm).

profiles machined to produce the gauge length between the profiles. The purpose of this was to give some strength and rigidity to the specimen to ensure handling did not prematurely fail the delicate gauge length. Once the specimen was mounted in the test machine, the central section was cut away using a miniature diamond wheel cutter to leave the only load path through the gauge length.

The specimens were cut from adhesive plaques that were cast between shimmed and polished aluminium plates which were coated with a release agent. The surface finish was seen to be good (only submicron metre scratches seen on specimen faces under the SEM), and specimens which contained visible voids in the gauge length were not included in the test programme. A single-pass milling cut was undertaken on each side of the specimens to ensure no steps were introduced on the cut edge. The edge finish after machining was seen to be similar to that on previous specimens which had not caused premature failure, and therefore no further machining or polishing was carried out on the specimens. The specimen gauge width and thickness were measured using a digital vernier caliper and a ball-ended micrometre. The nominal thickness for the large specimens was 2.3 mm (CoV 3.6%), 1 mm for the medium specimens (CoV 3.5%) and 0.5 mm for the small specimens (CoV 7.3%). The dimensions of the smallest specimens were measured using an instrumented optical microscope, giving digital readings with a resolution of 5 μm.

2.2. Specimen testing

The specimens were placed in a vacuum oven at 40°C. A control specimen from both the large and medium sample set was monitored for weight loss. It was seen that the mass had stabilized after 150 h in the oven, at which point it was assumed that the specimens were dry. The small specimens were too small to be monitored accurately for weight loss and were therefore given the same 150 h in the oven. Considering the much larger ratio of surface area to volume of the small specimens, the time to reach equilibrium will be shorter than for larger specimens, so 150 h was thought to be sufficient to be sure that a dry condition was reached.

All three specimen sizes were tested under displacement control, and the crosshead speed was adjusted to give a strain rate of 2.5% min^{-1} for each specimen size. The temperature of the specimens during test was monitored by the use of a thermocouple placed next to the specimens. It was seen that the temperature varied by only 2°C between the specimens, averaging at 22°C.

Alignment jigs were used to mount the specimens in the test machines to ensure that the gauge length was parallel to the direction of crosshead movement to reduce the possibility of bending. The jaws of the grips were set up with one dead jaw and one live jaw, the dead jaws having been aligned by the use of a very stiff piece of gauge plate, thereby minimizing the degree of bending of the specimen.

2.3. Extensometry

The smallest specimens were too small to be adequately monitored for strain by the standard techniques of strain gauging or clip-on extensometry. Furthermore, it has been shown experimentally [10] and theoretically [11] that strain gauges can affect low-modulus materials by artificial stiffening in the region around the gauge. This artifical stiffening can lead to both inaccurate determination of the stress–strain response, and to premature failure around the strain gauge. Clip-on extensometry is difficult to use for these materials owing to damage induced by the clip gauge knife edges. Consequently, a video extensometer system was used to monitor the strains. The system was originally developed in the University of Bristol Department of Computer Science to monitor displacements on a road bridge, but with minor modifications it was useful as a strain-measuring device. The system works by pattern matching a template drawn on to the specimen and following the template as the specimen deforms [12]. The distance between the template (in pixels on the CCD array) is then used to determine strain. The pattern-matching algorithm

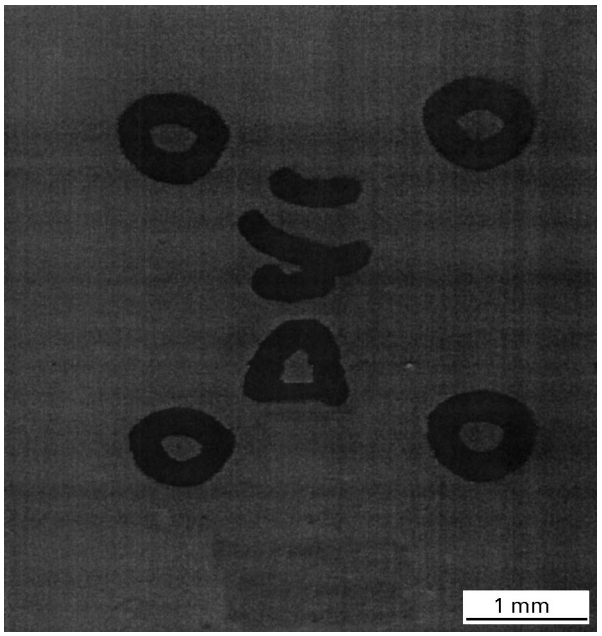

Figure 2 Specimen marking for tensile strain and Poisson's ratio, medium specimen 1.

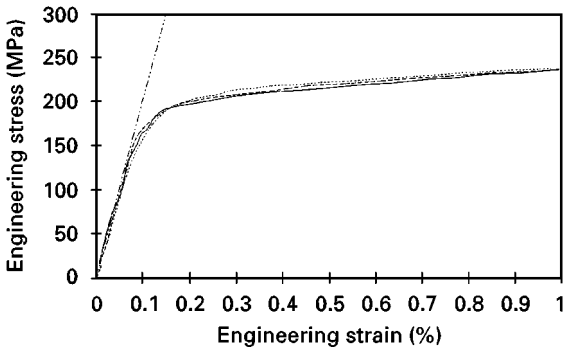

Figure 3 Comparison of video gauge, strain gauge and clip gauge on same steel specimen. (– · · –) 207 GPa theory, (——) vision system, (- - -) strain gauge, (---) clip gauge.

uses interpolation to give 1/25th pixel resolution in position in both the x and y directions. The use of two templates, therefore, gives uniaxial strain measurements, whilst the use of four templates in a square pattern gives Poisson's ratio as well as two uniaxial strains (allowing a check for in-plane bending of the specimen). The large and medium specimens were marked using an ink circle. The small specimens were too tiny for this and hence solid templates were used. Indian ink was used as the marking medium so as not to damage the adhesive. Fig. 2 details a screen shot of a medium specimen under test (specimen D1/1), and shows the specimen marking for Poisson's ratio. By the use of telephoto lenses, the physical scale of the specimen under test became irrelevant. Providing that the templates were placed as far apart on the screen as possible, the strain resolution was scale-invariant.

To determine the accuracy of the video extensometry system in comparison with strain gauges and clip gauges, a mild steel specimen was strain gauged, video gauged and clip gauged. Fig. 3 shows the tensile stress–strain curve from each method and it may be seen that very little difference exists between the methods. Steel was chosen because it has sufficiently high tensile modulus not to be adversely affected by the stiffening effect of the strain gauge.

3. Results

3.1. Stress–strain curve

All the specimens appeared to follow the same stress–strain curve; the exact point of failure on this curve was the only variable seen between the specimens. The stress–strain curve is significantly non-linear, with no apparent linear portion visible even at low strains. An example of the shape of the curve is shown in Fig. 4, the particular sample this curve represents failed at a tensile strain of 8.5%. All data are referenced to the original dimensions of the specimen, and is therefore referred to as engineering stress and engineering strain.

The shape of the curve can be seen to plateau at a stress of 62 MPa after approximately 4% tensile strain. Some evidence of softening in the stress–strain curve may be seen just prior to failure, although this softening was only present in the higher strain specimens. It was apparent from the 61 valid tests that there is no significant variation of the maximum stress with specimen size. The value of 62 MPa can therefore be defined as a material property, for the testing and environmental conditions used here.

Weibull analysis of the strains at failure for the three specimen sizes are shown in Fig. 5. The graphs were formed using median rank regression [13]. The quoted characteristic strains, η, and shape factors, m, are for the two parameter Weibull distribution. The critical coefficient of determination, r^2, is also given along with the number of valid tests, N. The fit to the two-parameter Weibull distribution is good for all three specimen sizes, with the characteristic failure strain increasing as specimen size reduces. The shape factor for the different specimen sizes may be seen to vary between 3.4 and 6.2. This is in approximate agreement with previous work [6] on epoxy resins, although it must be stated that this reference was concerned with investigation of a scale effect on strength for a linear elastic material; the results

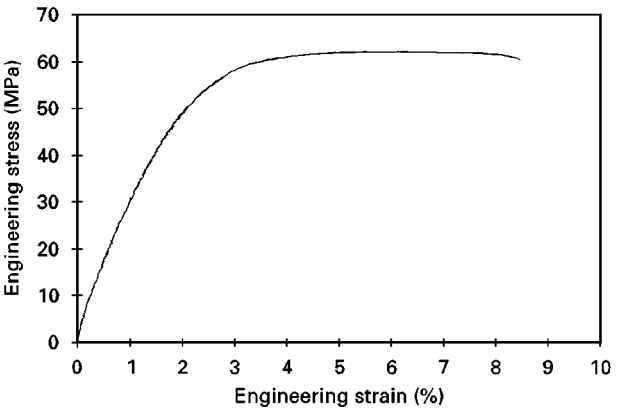

Figure 4 Typical engineering stress–Engineering strain curve for 3M EC3448 at RT dry condition.

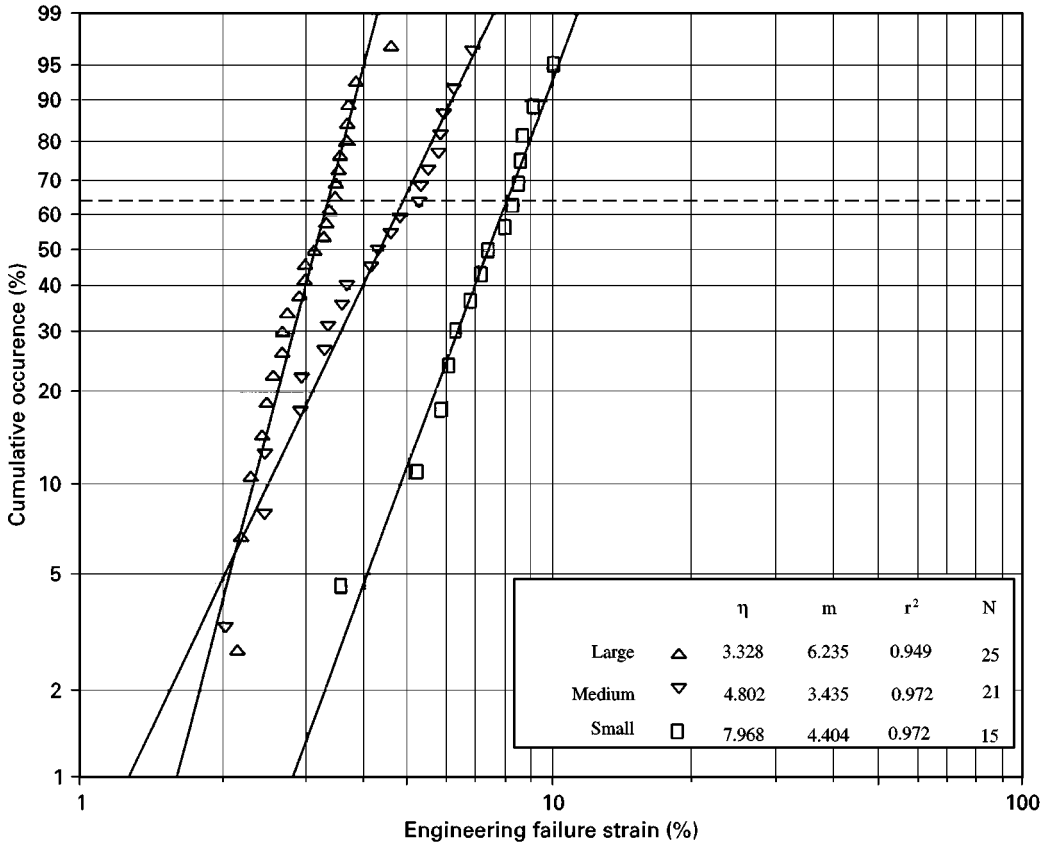

Figure 5 Weibull analysis for all tensile specimens of 3M EC3448. (△) large, $\eta = 3.328$, $m = 6.235$, $r^2 = 0.949$, $N = 25$ (▽) Medium, $\eta = 4.802$, $m = 3.435$, $r^2 = 0.972$, $N = 21$ (□) Small, $\eta = 7.968$, $m = 4.404$, $r^2 = 0.972$, $N = 15$.

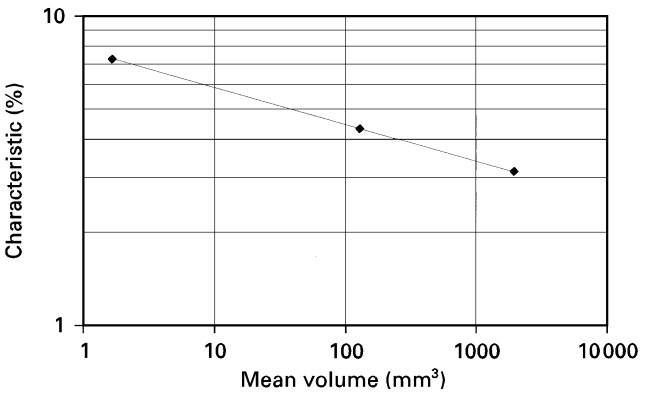

Figure 6 Weibull weak link scaling (WLS) diagram.

presented here show no such effect on strength but a scale effect on failure strain with approximately the same shape factor, *m*.

Using the characteristic strain and mean volume of the gauge section for each specimen size, a weakest link scaling diagram may be created, as shown in Fig. 6.

The gradient of a least-squares straight-line fit of the graph in Fig. 6 was used to determine a scaling shape factor, *m*, of 7.93. This value is higher than those for the scatter within each specimen size, but each sample set will be liable to errors from test and geometric variability. Assuming these errors to approximately equally to affect each specimen size, then the scaling diagram will remove these to leave only the material variability, hence a higher shape factor, *m*. This scaling value may be used to predict the increase or decrease in failure strain of a certain strained volume in comparison to another strained volume.

4. Failure analysis

4.1. Defect size

As each test was video-taped whilst using the video extensometer system, the images of each individual specimen during test could be viewed from the tape after the test had been completed. It was seen that whitening occurred in the specimen gauge length, with the severity of the whitening increasing as the specimen was strained. In all the specimen sizes, this whitening was generally seen to nucleate around distinct areas in the adhesive and gradually to propagate through the entire gauge length. Upon inspection of the failure surfaces after the test, it was seen that many of the large and medium samples showed defects present on the fracture surface, the majority of the defects being voidage. The small specimens generally showed no obvious defect in a low-powered optical microscope, although when using a scanning electron microscope (SEM) the defects could be seen. Whitening was visible on the fracture surfaces around the defects in the material, and hence could be attributed to the presence of defects. An instrumented microscope with 5 μm resolution was used to measure the dimensions of the defects that appeared to have initiated failure (voidage or non-voidage); as most of the defects were approximately ellipsoidal in shape, the major and minor axes of the ellipsoids were noted.

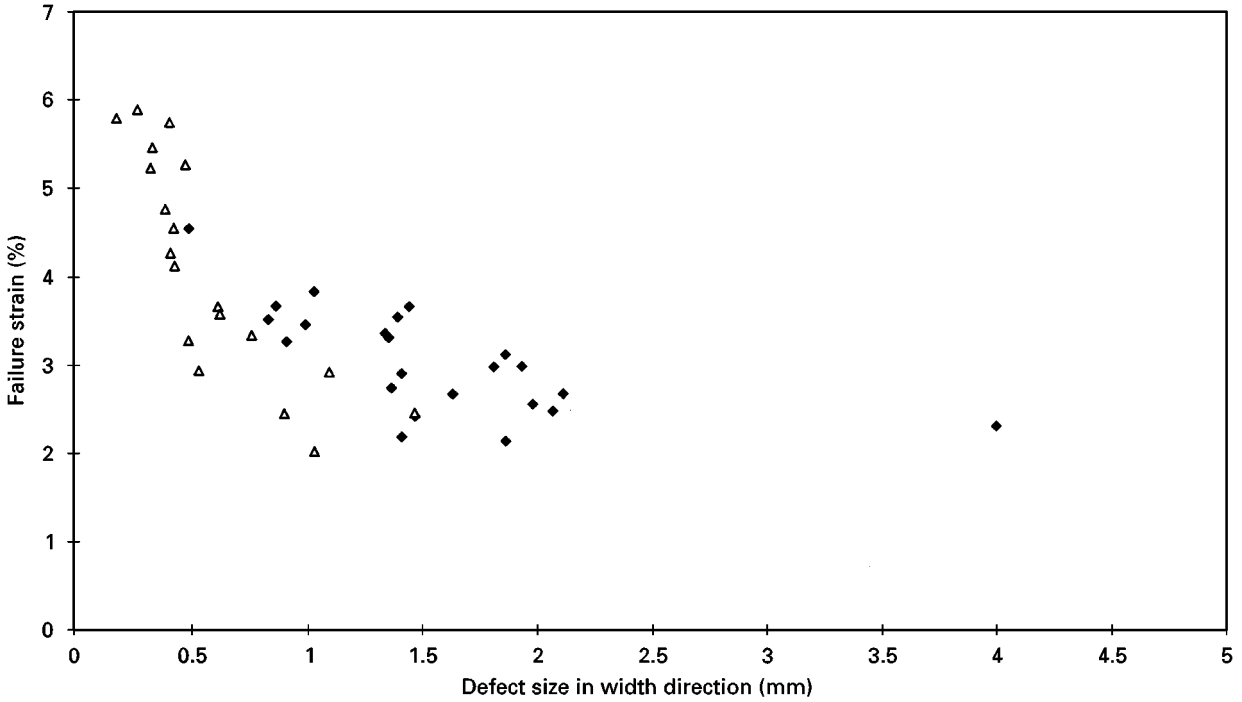

Figure 7 Variation of failure strain (%) with defect size (mm) in the specimen width direction, (◆) large specimens, (△) medium specimens.

Fig. 7 shows the correlation between tensile failure strain and defect size measured in the width direction of the specimens.

A trend of increasing strain to failure with smaller defect size is apparent from Fig. 7, although the large and medium specimens may be argued to lie on different curves. By expressing the defect size as a percentage of the available specimen width (10 mm for the large specimens and 5 mm for the medium specimens), Fig. 8 may be plotted.

The trend in Fig. 8 is similar to that in Fig. 7 but, by normalizing the data to specimen width, the large and medium specimens appear to lie on the same curve. The above data may be fitted to a power law curve of the form $\varepsilon = Ka^{-n}$ where ε is the tensile failure strain (%), K is some constant and a is the defect size (mm). This is shown in Fig. 9.

Highlighted in Fig. 9 are data points from eight specimens which failed from definable defects which were not voids. It may be seen that the dimensions of non-voidage defects to the corresponding failure strain fits the power-law approximation well, indicating that defects which are not voidage have the same effect on failure strain as a void of similar dimensions. This may be due to the non-voidage defects being inclusions, and therefore behaving in a similar manner to void which are not well bonded to the surrounding material.

Fig. 10 shows a void on the fracture surface, and Fig. 11 shows a specimen with a definable defect which was not voidage, as observed in the SEM. The defect in Fig. 11 is approximately circular with 1 mm diameter, situated in the centre of the figure.

The primary source of the voidage was the beading of the adhesive in the manufacture of the plates from which the specimens were cut, although some voidage was found to be present in the tubes. The non-voidage defects contained high concentrations of particulate silica which was not fully blended into the resin and formed particulate inclusions, or regions of higher than normal silica content.

4.2. Strain recovery

To investigate the nature of the strain recovery of the material after loading, the video images recorded during test were re-analysed using image analysis software to measure the distances between the targets during the test and just after failure to determine the degree of instantaneous strain recovery. Fig. 12 shows the results from a number of specimens, from the medium and small specimen sizes. The graph shows the residual strain present just after failure compared with the global failure strain of the specimen just before failure.

Also included in Fig. 12 are data from a number of cyclic tensile tests carried out on the adhesive at the large specimen size. Specimens were loaded in tension to various strain levels and then unloaded back to zero stress. The strain measured at this zero load level was recorded. The degree of instantaneous strain recovery can be seen to be great, up to approximately 6% for the specimens tested here. In view of the large strain recovery seen from Fig. 12, it may be concluded that the material is non-linear elastic to a large extent, with some permanent strain present immediately after failure. Considering the polymeric nature of the material, it is more applicable to quote the material response as viscoelastic = viscoplastic rather than classically elasto-plastic.

5. Implications for adhesive joint strength prediction

The material has been shown to have non-linear elastic properties to a large degree, and the tensile failure

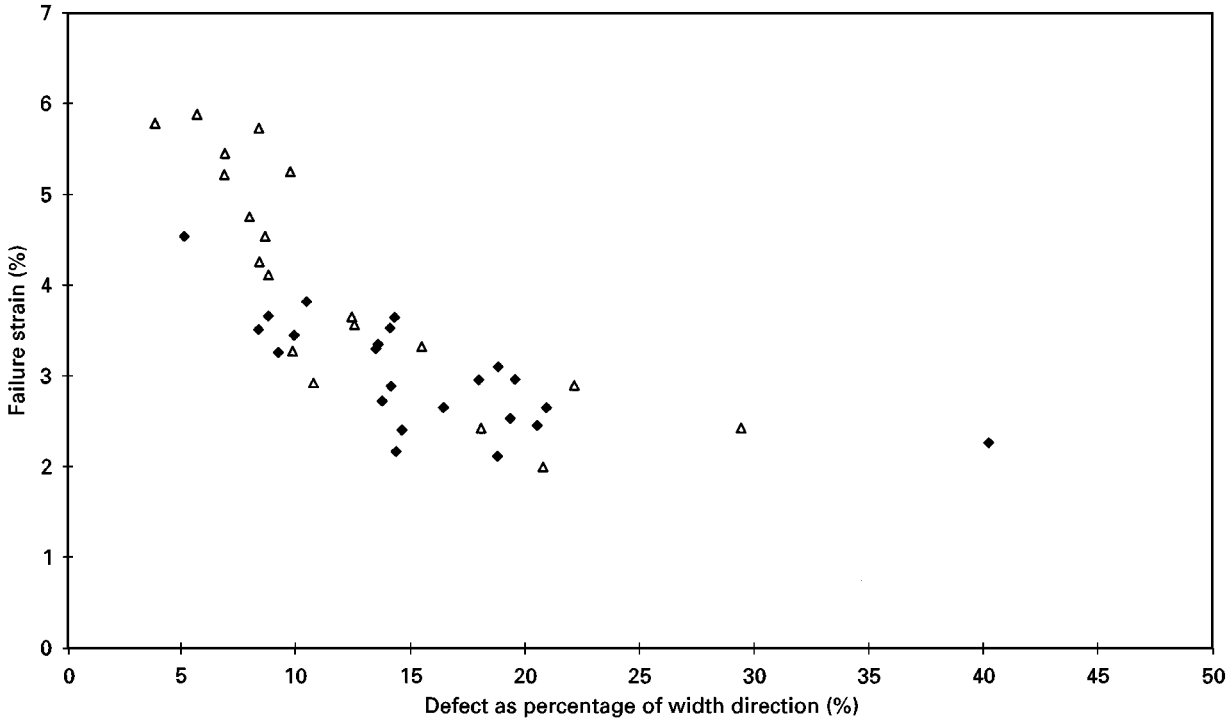

Figure 8 Failure strain to defect size as percentage of available specimen width. (◆) large specimens, (△) medium specimens.

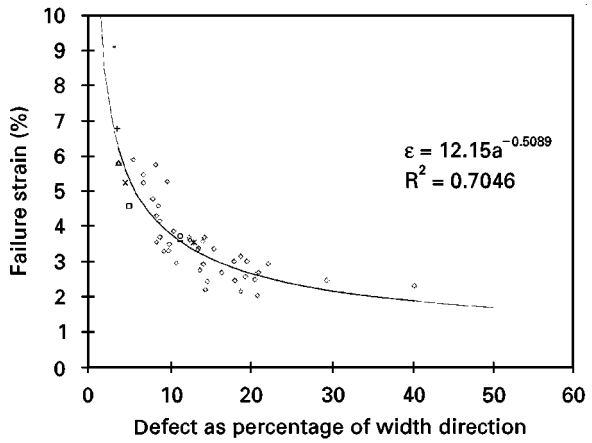

Figure 9 Power-law approximation to failure strain/defect size correlation; (◇) all voids, (○) large 6, (□) large 9, (+) medium 9, (△) medium 26, (×) medium 32, (∗) medium 33, (-) small 5, (−) small 8, (—) power fit.

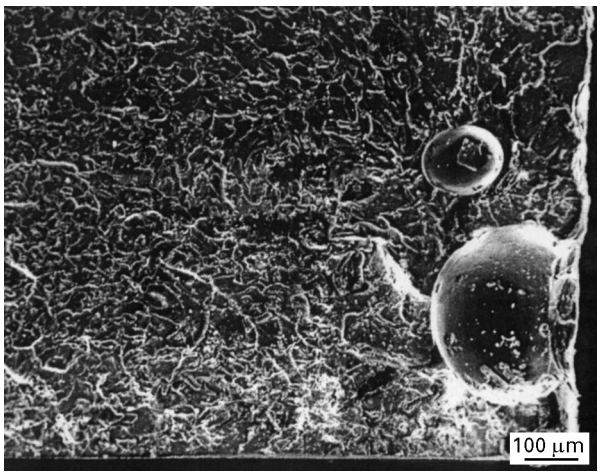

Figure 10 Typical voidage specimen observed in an SEM.

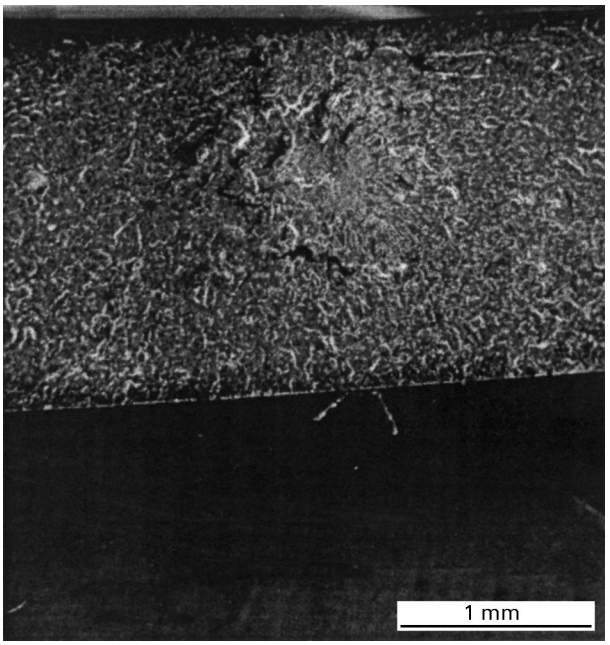

Figure 11 Non-voidage defect observed in an SEM.

strain to follow a Weibull distribution. Small specimens have been shown to have higher failure strains than larger specimens, the degree of the scale effect being relatively strong ($m = 7.9$). The correlation between failure strain and defect size has been seen to exist in accordance with the theories describing a defect sensitive material. Finally, the material has been shown to recover large amounts of strain after failure, indicating that the often used material model of elasto-plastic response is not applicable.

As mentioned in Section 1, discrepancies exist between the FEA predictions and what is observed in

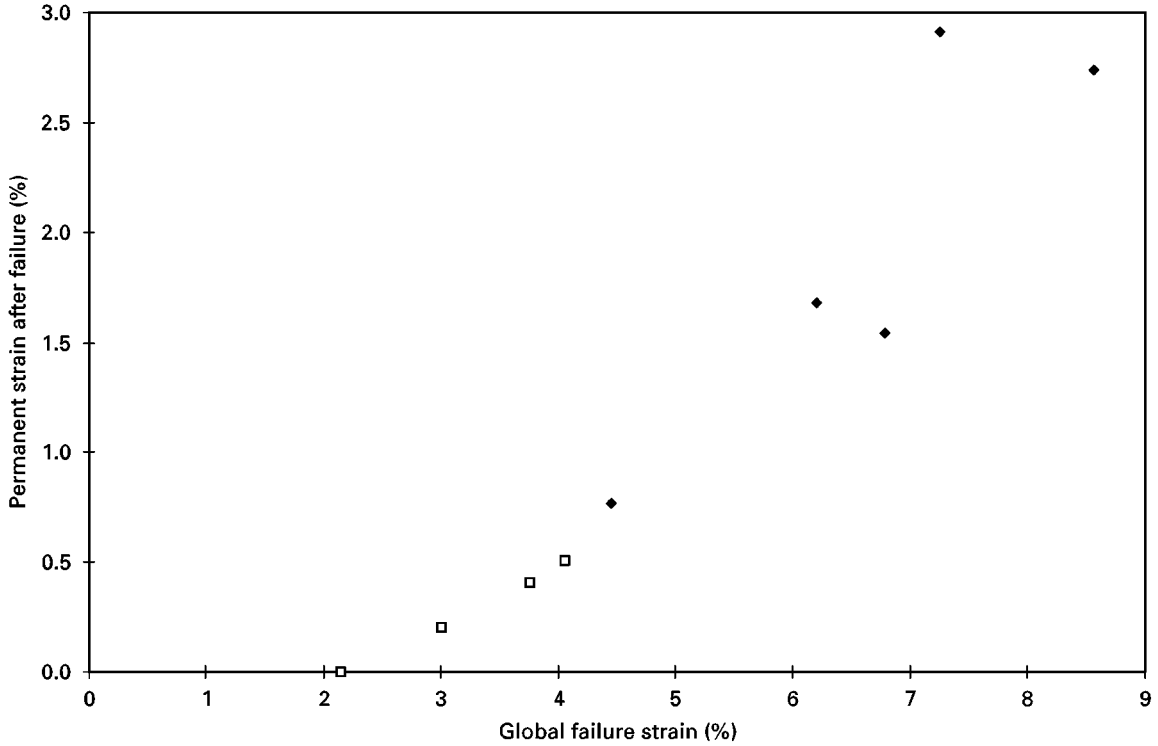

Figure 12 Strain at zero load versus global strain level (%); (◆) video stills, (□) cyclic testing.

practical adhesive joint testing. The primary problem areas are those of local geometry insensitivity and the ability of the adhesive to withstand very large strains in small volumes around the adherend tips. Both of these discrepancies are explained by the presence of a scale effect in the adhesive. The insensitivity to local geometry arises from the fact that small-scale changes in geometry may affect the peak strains produced, but only affect the material immediately around that small-scale geometry (by the principle of St Venant). Hence, the influence of small perturbations is ameliorated by the scale effect in the adhesive–the volume of material over which this changing strain acts may be small enough not to affect significantly the overall probability of failure of the joint. Only when these changes in geometry act over a larger region do the changes become important.

The second difficulty is that of the highly localized strains that are predicted by the FEA – historically it has been difficult to understand how the uncracked adhesive is capable of withstanding these high localized strains. This is also explained by the existence of a scale effect; the shape factor of 7.9 noted above may be used to quantify the failure strain of a highly localized volume of material in an adhesive joint.

Future work will concentrate on the use of the material parameters calculated above in the prediction of cohesive failure in adhesive joints.

6. Conclusion

Three specimen sizes of the 3M EC3448 single-part structural epoxy paste adhesive have been tested in tension. It was observed that the tensile failure strain increases with reducing specimen size, and the equivalent shape factor derived from a WLS chart being 7.9. Correlation was seen between the defect size and the tensile failure strain of the adhesive specimens, in a similar fashion to the trend observed in brittle materials.

It is therefore clear that the only tensile strength material property that may be stated for this material is the plateau stress level, although this, in itself, is likely to be dependent upon moisture content, test temperature and strain rate. The failure strain of the adhesive, or related quantities such as the energy stored in the specimen at failure, cannot be regarded as material constants without specific reference to both the defect spectrum that is contained within the specimen and the specimen size.

Failure prediction of adhesively bonded joints of this material under these environmental and testing conditions must therefore take into account the scale sensitivity of the adhesive as the distribution of stress within the joint very often leads to localized strains, and small adhesive volumes have been shown to have higher failure strains than standard adhesive testpieces.

References

1. J. A. HARRIS and R. D. ADAMS, *Int. J. Adhes. Adhesives* **4** (1984) 65.
2. J. D. CLARKE and I. J. McGREGOR, *J. Adhes.* **42** (1993) 227.
3. A. D. CROCOMBE, *Int. J. Adhes. Adhesives* **9** (1989) 145.
4. R. D. ADAMS and J. A. HARRIS *ibid.* **7** (1987) 69.
5. M. IMANAKA, K. HARAGA and T. NISHIKAWA, *J. Soc. Mater. Sci. Jpn.* **41** (1992) 1662.
6. E. M. ODOM and D. F. ADAMS, *J. Mater. Sci.* **27** (1992) 1767.
7. M. R. WISNOM and M. I. JONES, *J. Reinf. Plastics Compos.* **15** (1996) 2.
8. T. K. O'BRIEN and S. A. SALPEKAR, *Compos. Mater. Test. Design* **11** (1993) 23.

9. H. L. HARTER, Air Force Flight Dynamics Laboratory, OH, USA, Report AFFDL-TR-77-11 (1976).
10. B. C. DUNCAN and P. E. TOMLINS, MTS Adhesives Project 1, Report 2 (1994) National Physical Laboratory, UK.
11. C. C. PERRY, "Manual on Experimental Methods for Mechanical Testing of Composites" (Elsevier Applied Science, London, 1989) p. 35.
12. A. TOWSE, *J. Strain Anal.* Submitted.
13. R. B. ABERNETHY, "The New Weibull Handbook", 2nd, Edn (Abernethy, Palm Beach, FL, 1996).

Received 21 April
and accepted 15 May 1998